In vivo localization at the cellular level of stilbene fluorescence induced by Plasmopara viticola in grapevine leaves.

Sébastien Bellow, Gwendal Latouche, Spencer C Brown, Anne Poutaraud, Zoran G Cerovic

Journal of Experimental Botany, Vol. 63, No. 10, pp. 3697–3708, 2012
doi:10.1093/jxb/ers060 Advance Access publication 12 March, 2012
This paper is available online free of all access charges (see http://jxb.oxfordjournals.org/open_access.html for further details)

Journal of Experimental Botany
www.jxb.oxfordjournals.org

RESEARCH PAPER

In vivo localization at the cellular level of stilbene fluorescence induced by *Plasmopara viticola* in grapevine leaves

Sébastien Bellow[1], Gwendal Latouche[1], Spencer C. Brown[2], Anne Poutaraud[3] and Zoran G. Cerovic[1,*]

[1] Univ Paris-Sud, Laboratoire Écologie Systématique et Évolution, CNRS UMR 8079, Bât. 362, 91405 Orsay, France
[2] Institut des Sciences du Végétal, CNRS UPR 2355 & FRC3115, 91198 Gif-sur-Yvette, France
[3] INRA, UMR 1131 Santé de la Vigne et Qualité du Vin, 68000 Colmar, France

* To whom correspondence should be addressed. E-mail: zoran.cerovic@u-psud.fr

Received 9 December 2011; Revised 2 February 2012; Accepted 6 February 2012

Abstract

Accurate localization of phytoalexins is a key for better understanding their role. This work aims to localize stilbenes, the main phytoalexins of grapevine. The cellular localization of stilbene fluorescence induced by *Plasmopara viticola*, the agent of downy mildew, was determined in grapevine leaves of very susceptible, susceptible, and partially resistant genotypes during infection. Laser scanning confocal microscopy and micro-spectrofluorimetry were used to acquire UV-excited autofluorescence three-dimensional images and spectra of grapevine leaves 5–6 days after inoculation. This noninvasive technique of investigation *in vivo* was completed with *in vitro* spectrofluorimetric studies on pure stilbenes as their fluorescence is largely affected by the physicochemical environment in various leaf compartments. Viscosity was the major physicochemical factor influencing stilbene fluorescence intensity, modifying fluorescence yield by more than two orders of magnitude. Striking differences in the localization of stilbene fluorescence induced by *P. viticola* were observed between the different genotypes. All inoculated genotypes displayed stilbene fluorescence in cell walls of guard cells and periclinal cell walls of epidermal cells. Higher fluorescence intensity was observed in guard-cell walls than in any other compartment due to increased local viscosity. In addition stilbene fluorescence was found in epidermal cell vacuoles of the susceptible genotype and in the infected spongy parenchyma of the partially resistant genotype. The very susceptible genotype was devoid of fluorescence both in the epidermal vacuoles and the mesophyll. This strongly suggests that the resistance of grapevine leaves to *P. viticola* is correlated with the pattern of localization of induced stilbenes in host tissues.

Key words: 3D fluorescence microscopy imaging, autofluorescence, defence response, downy mildew, phytoalexins, resistance to pathogen, resveratrol, spectrofluorimetry, Vitaceae (*Vitis vinifera L.*).

Introduction

Downy mildew is a severe disease of grapevine, one of the most cultivated plants in Europe. *Plasmopara viticola* (Berk. & Curt.) Berl. & de Toni, the oomycete responsible for this infection, attacks all green parts of grapevine, leads to a decrease of grape yields and alters the quality of wine produced. The defence response of plants against biotic or abiotic stresses involves either preformed constitutive defences (Vance *et al.*, 1980) or induced active mechanisms (Harborne, 1999). The induction of biosynthesis and accumulation of phytoalexins falls in the category of active defence (Kuc, 1995; Hammerschmidt, 1999). Thirty years ago, Langcake first identified stilbenes as phytoalexins of grapevine and then showed some key features of these phenolic compounds (Langcake and Pryce, 1976, 1977; Langcake *et al.*, 1979; Langcake, 1981).

During the last 30 years, many studies have sought to understand the antifungal activities of stilbenes. These phytoalexins were shown to reduce the germination of *Botrytis*

cinerea conidia (Langcake and Pryce, 1976; Langcake, 1981; Hoos and Blaich, 1990) or of *P. viticola* sporangiophores and to reduce the mobility of zoospores (Pezet *et al.*, 1994). These *in vitro* studies were an ersatz to studies on mycelia because *in vitro* experiments are not possible on *P. viticola* mycelium, which is an obligatory biotroph. Susceptible grapevine species infected by *P. viticola* mainly produce *trans*-resveratrol (3,5,4'-trihydroxystilbene) and *trans*- and *cis*-piceid (3-*O*-β-D-glucoside of resveratrol) (Pezet *et al.*, 1994) whereas resistant species produce *trans*-resveratrol, *trans*-pterostilbene (3,5-dimethoxy-4'-hydroxystilbene) and cyclic dehydrodimers of resveratrol *trans*-ε-viniferin and *trans*-δ-viniferin (Langcake, 1981; Dercks and Creasy, 1989; Pezet *et al.*, 2003). This result is corroborated by the fact that distinctive toxicities to *P. viticola* zoospores were reported for these stilbenes (Pezet *et al.*, 2004a, b). The highest concentrations of viniferins appear in resistant cultivars and they correlate with growth inhibition of *Erysiphe necator* (powdery mildew) (Schnee *et al.*, 2008). Similarly, an inhibition of the growth of *P. viticola* was observed *in vivo* on resistant cultivars producing viniferins and/or pterostilbene (Alonso-Villaverde *et al.*, 2011). All these results suggest that stilbenes are implicated in the resistance of grapevine to fungi. Yet, the effect of stilbenes on mycelia of the biotrophic agent *P. viticola* remains a matter of debate (Chong *et al.*, 2009) and obviously needs more investigation *in vivo*. No physical, biochemical, or genetic evidence of the direct interaction between plant-induced stilbenes and mycelium *in situ* is currently available. Despite the lack of direct evidence, the production of stilbenes was reported to correlate well with resistance levels to pathogens in *Vitis* species (Chong *et al.*, 2009). Therefore, the quantitative and qualitative (chemical) detection of stilbenes is used to screen disease-resistant genotypes in breeding programmes (Pool *et al.*, 1981; Jeandet *et al.*, 1995; Gindro *et al.*, 2006; Shiraishi *et al.*, 2010).

Stilbenes are fluorescent under UV light, emitting violet-blue fluorescence (Hillis and Ishikura, 1968) with an excitation peak around 320 nm and an emission peak at 390 nm in methanol as well as in leaves (Poutaraud *et al.*, 2007). Fluorimetry is therefore a potential *in vivo* approach to analyse naturally occurring stilbene (Poutaraud *et al.*, 2007; Poutaraud *et al.*, 2010). Epifluorescence microscopy allowed the observation of intrinsic fluorescence of stilbenes in epidermal cell walls and guard cells (Dai *et al.*, 1995a, b). Fluorimetry has served to assess stilbenes *in vivo* in grapevine leaves: a positive correlation was found between the UV-induced violet-blue fluorescence on both abaxial and adaxial surfaces of leaves, at a macroscopic scale, and the stilbene content measured by HPLC coupled to photodiode array detectors (absorption spectra) in the extract corresponding to the measured leaf area (Poutaraud *et al.*, 2007). Hence, the local stilbene autofluorescence can be used to probe the grapevine leaf–*P. viticola* interaction at a microscopic scale (Poutaraud *et al.*, 2007). The latter fluorimetric study was performed on susceptible cultivars and only assessed the autofluorescence of leaf surfaces. Langcake and Lovell (1980) suggested that stilbenes are located immediately around the lesion and might inhibit the growth of *P. viticola* when produced at the right time and the appropriate site. Their hypothesis of stilbene involvement in the defence response of resistant genotypes implies their localization in the mesophyll, where hyphae fully develop. Yet, as Langcake (1981) admitted, the antifungal activities of stilbenes against the obligatory parasite *P. viticola* would be difficult to prove.

Mechanisms regulating the synthesis of stilbenes are complex (Chong *et al.*, 2009). Thus, investigations on stilbenes themselves in addition to those on stilbene synthase (Fornara *et al.*, 2008; Wang *et al.*, 2010) and its genes (Jaillon *et al.*, 2007) are required to elucidate these mechanisms. *Vitis* cell suspension culture is a useful and interesting model to study these mechanisms but limited by its *ex situ* nature (Donnez *et al.*, 2009).

One key in understanding the host–pathogen interaction is nondestructive investigation of deep tissues *in situ*. Therefore, this study undertook a noninvasive *in vivo* microscopic and microspectrofluorimetric three dimensional (3D) investigation by confocal laser scanning microscopy of *P. viticola*-induced stilbene fluorescence in grapevine leaves. As shown by Hutzler *et al.* (1998), this technique enables *in vivo* visualization of phenolic compounds inside leaves by 3D reconstructions and optical sections. It makes it possible to obtain information about the subcellular localization of these compounds and quantitative information about their fluorescence intensity. By localizing stilbenes during pathogenesis, the aim is to better understand the role of these phytoalexins in defence reactions against *P. viticola*. Yet the various leaf compartments are known to have different physicochemical characteristics that can influence stilbene fluorescence. Therefore, there were three objectives of this study: (1) to acquire 3D fluorescence images of infected and control leaves; (2) to compare three genotypes with different degrees of susceptibility; and (3) to understand physicochemical characteristics of stilbene fluorescence as factors affecting the patterns observed in tissue *in vivo*.

Materials and methods

Plant material and artificial infection

Three genotypes of grapevines of different degrees of susceptibility to *P. viticola* were used: two *Vitis vinifera* cv. (Muscat Ottonel and Cabernet Sauvignon) and one hybrid (RV1), which are very susceptible, susceptible and partially resistant, respectively, to *P. viticola*. The hybrid is a crossing of the American species *Muscadinia rotundifolia* with several *V. vinifera* cultivars. It carries the resistance allele *Rpv1* (Merdinoglu *et al.*, 2003). Plants were grown from green cuttings in Colmar (France) at 22 ± 3 °C with 13/11 light/dark in the greenhouse. The study was performed on plants at the stage of about 15 leaves. *P. viticola* was obtained from naturally infected plants in Colmar. Sporangia were periodically grown in order to prepare inoculants. Sporangia were diluted in distilled water, counted, and then adjusted to a concentration of approximately 10^5 sporangia ml^{-1}. The fifth leaf from the apex was detached and inoculated with the abaxial side floating on the *P. viticola* inoculum suspension during 5 h in darkness. The sixth leaf was also detached to be used as control and was immersed 5 h in distilled water instead of the inoculum suspension. After treatments, the leaves were put in 14-cm diameter Petri dishes with the adaxial side against wet paper and maintained under moist conditions to favour the sporulation. Time is denoted days post inoculation (dpi).

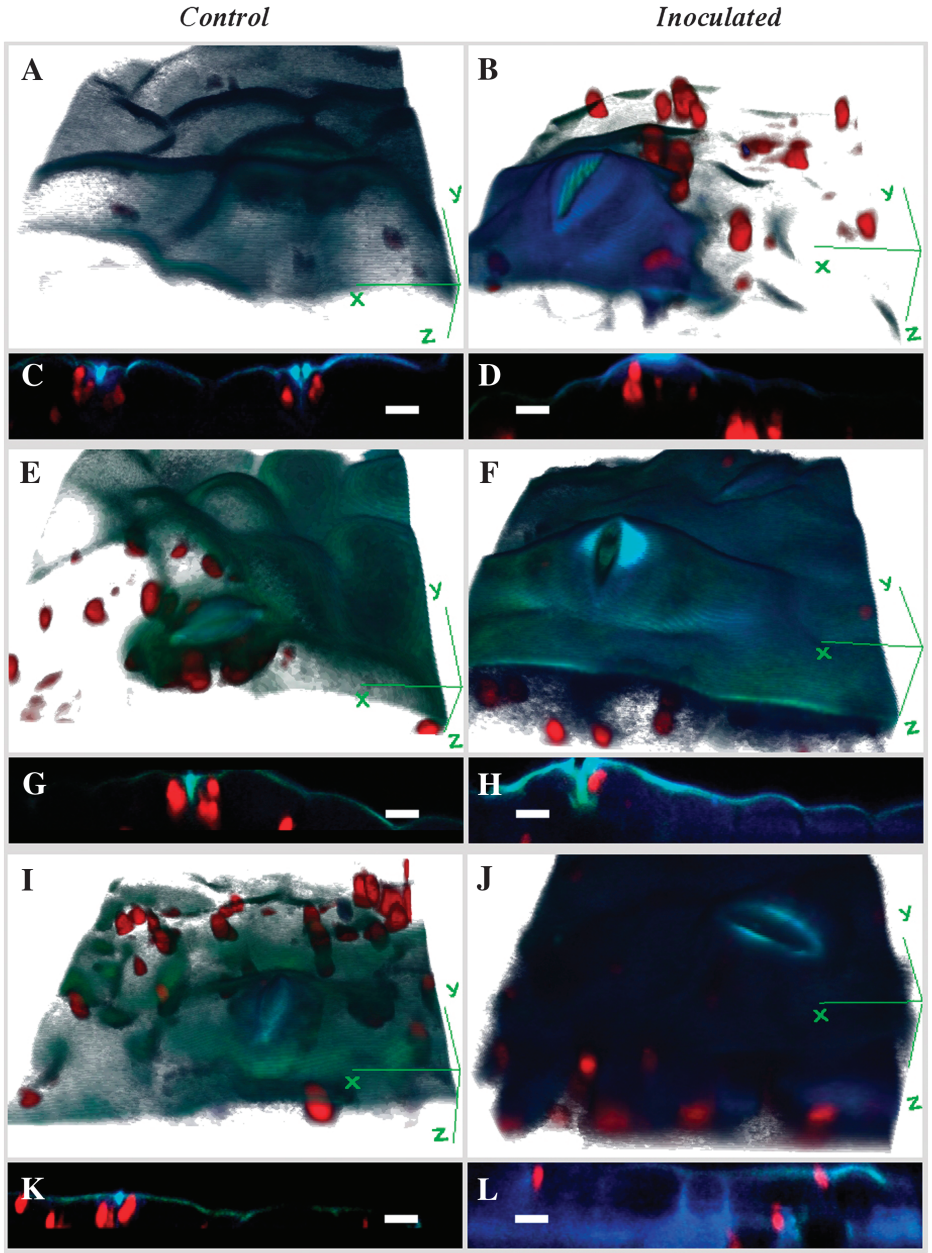

Fig. 1. Autofluorescence microscopy under UV excitation (351 nm) of control (left) and inoculated (right) leaves of *V. vinifera* cv. Muscat Ottonel (A–D) and Cabernet Sauvignon (E–H), very susceptible and susceptible to *P. viticola*, respectively, and of the partially resistant hybrid RV1 (I–L). Inoculated samples were analysed at 5 dpi for Muscat Ottonel and Cabernet Sauvignon and at 6 dpi for RV1. Here are represented, for each sample, the 3D projection (oriented abaxial side up) and an orthogonal view (optical section) extracted from the Z-stack. Each image couple (control and inoculated) is a red/green/blue colour overlay shown under the same fluorescence intensity settings. 3D images represent an area of approximately 71 × 71 μm^2 and green lines show the scanning coordinates. Bars, 20 μm. Leaf fragments were mounted in microscopy oil. 3D animations are available in Supplementary Videos S1–S3.

Confocal microscopy and 3D image reconstruction

The confocal microscope (LSM510 Meta, Zeiss, Jena, Germany) had an argon-ion laser (Enterprise II, Coherent, Santa Clara, CA, USA) providing wavelengths of 351 and 364 nm dynamically filtered by an acousto-optic tunable filter (AOTF). All experiments were performed with a ×63 objective (Plan-Apochromat, NA 1.40 oil, Zeiss) and at room temperature (19 °C). Grapevine leaf autofluorescence was excited at 351 nm (wavelength being closer to the 320 nm peak of stilbenes). The dichroic filters used were HFT UV/488 (Zeiss) for standard imaging and HFT UV (375) (Zeiss) for microspectrofluorimetry, the latter being fairly flat from 375 to 800 nm. For all image acquisitions, the AOTF was set to 50% and the detector pinhole to 82 μm. Different gains of detectors had to be used for optimal acquisition: these settings were recorded and appropriate corrections were applied (after calibration) to be able to compare images on the same intensity scale. Leaf fragments were mounted in oil for microscopy (Immersol 518N, Zeiss) with abaxial side facing the objective. The cover slips thickness was 0.170 mm (#1.5).

The array detector of the Zeiss LSM510 Meta is a spectrograph dispersing emitted fluorescence from 361.8 nm to 704.2 nm on a 32 photo-multiplier tube (PMT) array. The 32 signals were either selectively binned for standard imaging or recorded individually for microspectrofluorimetry. The images presented in this paper are the

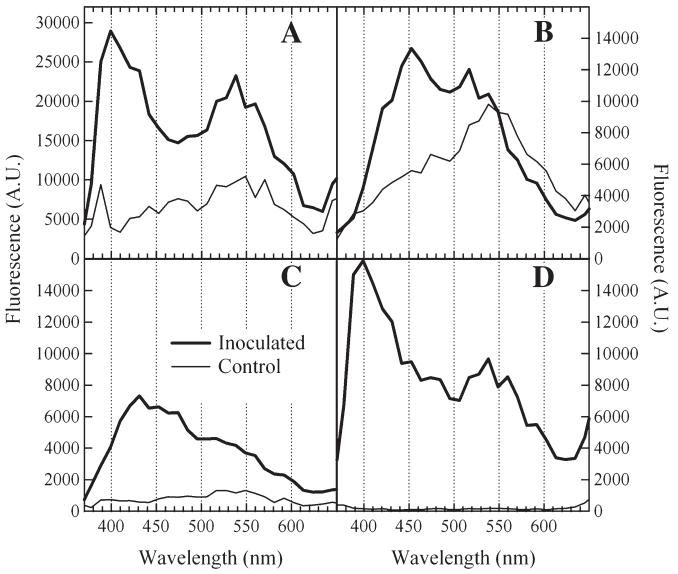

Fig. 2. Fluorescence emission spectra (excitation 351 nm) emitted from different regions of the control (thin line) and inoculated (bold line) leaves of Muscat Ottonel at 5 dpi (A, B), Cabernet Sauvignon at 5 dpi (C), and RV1 at 6 dpi (D). The fluorescence emission spectra of 3D regions of interest (ROI), that were obtained from the 4D acquisitions (see Materials and methods for details), were respectively localized on the surface of guard cells delimiting stomata (A), on the surface of epidermal cells (B), in the volume of epidermal cell vacuoles (C), and in the spongy mesophyll volume (D). Each curve is the mean of all pixels of the ROI. The Raman emission of water (excitation 351 nm, emission 399 nm) is not detectable in this configuration.

overlay of three detection channels on the Meta array detector: 361.8–479.5 nm (blue channel), 500.9–597.2 nm (green channel), and 629.3–682.8 nm (red channel). An averaging of four frames and a pixel dwell time of 1.20 µs was used. Series of XY images, called Z-stack, were acquired along the Z axis, the axis perpendicular to leaf samples surface and parallel to the excitation beam. The optimal voxel size of 0.13 × 0.13 × 0.60 µm, for x, y and z directions, respectively, was used. The resolution of the acquired images was 1024 × 1024 pixels coded in 8 bits for each colour channel. For fluorescence intensity comparison, intensity scales of each of the channels (blue, green, red) were equalized between images of inoculated and control samples of a given genotype before the overlay. The Z-stacks allowed a 3D analysis that is shown here through 3D projections and optical sections (orthogonal projections). Image acquisition was performed using the software Zen (Zeiss), and image analysis, including 3D reconstruction, was performed using the software LSM Image Browser (Zeiss) and the program ImageJ (http://rsbweb.nih.gov/ij/). The presented results (Figs. 1, 2, and 3) are representative of several experiments. Each of them was repeated at least twice for each genotype and in two different years. Trials on other confocal systems, including two-photon excitation, were unsatisfactory due to loss of emission below 400 nm.

Microspectrofluorimetry

The LSM510 Meta confocal microscope has a spectral mode able to acquire fluorescence emission spectra between 361.8 and 704.2 nm using the 32 PMT (10.7 nm bandwidth). In this study, emission spectra were acquired between 362 and 694 nm (24 bands) for every pixel during a Z-stack acquisition. In these 4D acquisitions (spectral + Z-stack) the resolution was limited to 512 × 512 pixels, so the voxel sizes of the 4D acquisitions was increased to 0.26 × 0.26 × 0.60 µm and the pixel dwell time was 1.6 µs. Using the 4D data, fluorescence emission spectra of 3D regions of interest were obtained. Analysis of the spectra was performed with ImageJ, LSM Image Browser, and the numerical/graphic program Igor 6 (WaveMetrics, Lake Oswego, Oregon).

Fluorescence spectroscopy

Fluorescence excitation and emission spectra of *trans*-resveratrol, *trans*-pterostilbene, and *trans*-piceid in solution (10 µM) were recorded with a spectrofluorimeter (Cary Eclipse, Varian, Les Ulis, France) in a 90° configuration at 20 °C. Quartz cells of 1-cm path-length (111-QS, Hellma, Paris, France) were used. Excitation spectra were corrected with a calibrated photodiode (S1337–1010BQ, Hamamatsu, Massy, France), and emission spectra were corrected using a standard lamp with a known spectrum (LI-COR 1800–02) as described in detail previously (Louis *et al.*, 2006). In addition, corrected spectra were expressed in quinine sulphate equivalent units (QSEU) as practised by Cerovic *et al.* (1999): 1000 QSEU correspond to the fluorescence of 1 µM quinine sulphate dihydrate in 0.105 M perchloric acid for 1-cm light path square cells or, in general, 1 nmol cm^{-2}, excited at 347.5 nm and with an emission at 450 nm, under the identical conditions used to acquire the sample fluorescence spectrum. The fluorophores used were *trans*-resveratrol (R5010, Sigma-Aldrich, Saint Quentin Fallavier, France), *trans*-piceid (4992, Extrasynthese, Lyon, France), *trans*-pterostilbene (P1499, Sigma-Aldrich), and quinine sulphate dehydrate (99.0%, Fluka 22640, Sigma-Aldrich). The highest purity commercially available products were used for the solvents: ethanol (Fluka, Saint-Quentin, France), methanol (Merck, Darmstadt, Germany), propan-2-ol (Merck), ethylacetate (Sigma-Aldrich, Saint-Quentin, France), glycerol (Acros Organics, Geel, Belgium), water (Milli-Q, Millipore, Billerica, MA, USA), and chloroform (Baker, Deventer, Netherlands).

Results

In vivo *fluorescence confocal microscopy of grapevine leaves*

Presented images were acquired on three different genotypes of *Vitis vinifera*: cultivar Muscat Ottonel, very susceptible to *P. viticola*, Cabernet Sauvignon, a susceptible cultivar, and the partially resistant hybrid RV1. Although here leaves were detached, parallel observations by fluorescence macroscopy of leaves attached on whole plants were coherent with these observations (data not shown).

Sporulation confirmed the success of the artificial *P. viticola* inoculation, at 5 dpi and often earlier for very susceptible genotype, at 5 dpi for the susceptible genotype, and at 6 dpi for the partially resistant hybrid. The presence of sporulation is also a guarantee for the colonization of the mesophyll by *P. viticola* mycelium. On inoculated samples, microscopic observations were made on areas with sporangiophores and sporangia overlying stomatic cavities full of pathogen. Accordingly, the underlying mesophyll was infected. Under UV illumination, the abaxial surface of control grapevine leaves emitted two types of autofluorescence (Fig. 1): (1) the red fluorescence of chlorophyll in chloroplasts, which are present in both guard cells (GC) and spongy parenchyma cells of the mesophyll; and (2) the blue-green fluorescence (BGF) of the periclinal (parallel to the surface) epidermal cells (EC) and GC cell walls attributed to hydroxycinnamic acids (Cerovic *et al.*, 1999; Pfündel *et al.*, 2006). Inoculated grapevine leaf samples of the three genotypes displayed an increase in the BGF at the surface of GC in comparison to control samples (Fig. 1). The

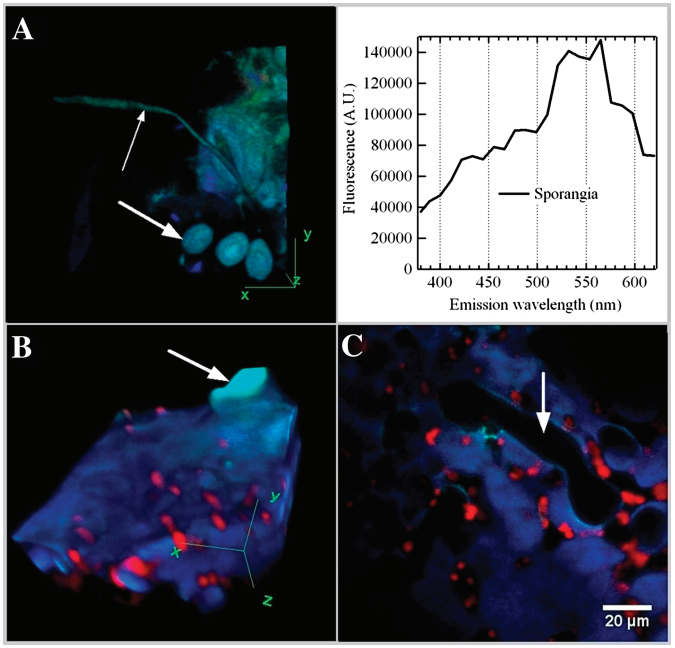

Fig. 3. Autofluorescence microscopy under UV excitation (351 nm) of inoculated leaves. (A) Sporulation structures, sporangia (thick arrow), and sporangiophores (thin arrow), on the abaxial surface of the very susceptible cultivar of *V. vinifera* Muscat Ottonel at 8 dpi and the fluorescence emission spectrum of the sporangia. (B) Fluorescence at the abaxial surface of the resistant hybrid RV1 with the eruption of a sporulation structure from a stoma (arrow) at 6 dpi. (C) Fluorescence of the mesophyll of RV1 at 6 dpi, showing an area in the mesophyll with no autofluorescence, most likely filled with mycelium (arrow). Same intensity scale as in Fig. 1. Images A and B represent an area of approximately 71 × 71 µm^2 and green lines show the scanning coordinates. Animations are available in Supplementary Video S4.

same was observed in periclinal EC cell walls. This increase in BGF of the cell walls at the abaxial leaf surface is due to the autofluorescence of induced stilbenes as previously reported (Poutaraud *et al.*, 2007). In addition, both the 3D projection of the Z-stack and the orthogonal cross section view of the inoculated Cabernet Sauvignon samples show a BGF in the lumen of EC at 5 dpi (Fig. 1F, H). The diffuse BGF of the EC lumen was very weak in the control Cabernet Sauvignon sample and was totally absent in the other genotypes, whether inoculated or control. The inoculated sample of the partially resistant genotype RV1 displayed a strong BGF located in the mesophyll (Fig. 1J, L). This strong BGF in the spongy parenchyma and in the intercellular space in the epidermis visible at 6 dpi was observed only on the inoculated samples of RV1 and not in any other samples. Supplementary Videos S1, S2, and S3 (available at *JXB* online) present the volume reconstructions of control and infected tissues from each genotype (cf. Fig. 1).

In vivo *microspectrofluorimetry of grapevine leaves*

Fig. 2 presents the fluorescence emission spectra of the structures seen in Fig. 1 acquired with the confocal microscope. The results shown in Fig. 2A and B were obtained on the GC and EC cell walls of Muscat Ottonel. Similar results were obtained with Cabernet Sauvignon and RV1 (data not shown). With UV excitation, periclinal cell walls of control leaves displayed a broad fluorescence emission spectrum with a maximum around 550 nm. Previous spectrofluorimetric studies performed at macroscopic scales reported a 450 nm peak of control grapevine leaves excited by UV (Cerovic *et al.*, 1999; Poutaraud *et al.*, 2007). This autofluorescence was attributed to hydroxycinnamic acids in particular since their *in vitro* emission has a peak around 420 nm (Cerovic *et al.*, 1999; Meyer *et al.*, 2003). In the present microspectrofluorimetric study, an additional '550 nm peak' was observed. The origin of this increase in green autofluorescence, which was seen before macroscopically only in the form of a small shoulder on the spectra, could not be explained (Cerovic *et al.*, 1999; Poutaraud *et al.*, 2007). This green fluorescence increased with inoculation more than would be expected from the tail of stilbene fluorescence in all inoculated samples, and it is even seen as a second peak in some cases (Fig. 2A, D). The '550 nm peak' is probably not a photobleaching artifact because under the experimental conditions (50% power at 351 nm, 4 frames averages) the images and emission spectra were quite stable and no significant differences were observed in the shape of spectra before and after Z-stack acquisition.

Considering the BGF spectra, two phenomena occurred upon inoculation. First, the fluorescence emission increased in the blue-green part of the spectra of all inoculated grapevine leaves (Fig. 2), and it was about 1.5 times stronger in GC than in EC cell walls (+51% versus +36% of the fluorescence spectra integrals). Second, on GC cutinized cell walls and mesophyll intercellular space (Fig. 2A, D), a peak emerged at 400 nm in accordance with the induction and accumulation of stilbenes (Poutaraud *et al.*, 2007). At 6 dpi, the spectrum acquired in the mesophyll of inoculated RV1 confirmed the strong BGF imaged with the confocal microscope (Fig. 1L). In all cases, the autofluorescence induced in inoculated samples can be attributed to a new fluorophore because it was always characterized by the appearance of a new fluorescence emission peak. In inoculated samples, the new peak due to the accumulation of stilbenes is at 400 nm (Fig. 2A, D), at 430 nm (Fig. 2C, vacuoles of EC), or at 450 nm (Fig. 2B, EC cell walls).

Autofluorescence of P.viticola

Upon infection by *P. viticola,* surface hyphae and sporangiophores bearing sporangia emerge through the stomata at the abaxial side of inoculated leaves. Fluorescence microscopy under UV excitation revealed that the pathogen structures developing at the abaxial surface of grapevine leaves are autofluorescent and display a BGF (Fig. 3A). Emission spectra of these aerial fungal structures had a maximum around 550 nm, close to the emission spectra of the underlying cell walls (Fig. 3A). However, for all genotypes, the subepidermal pathogen structures were not visible under UV excitation. Hence, the 3D reconstruction of UV excited

fluorescence of infected tissues did not allow the direct observation of the colonization of mesophyll by *P. viticola*. Indeed, in RV1, which displayed a strong intercellular BGF in the spongy parenchyma (Fig. 1J, L), the mycelium colonization can be deduced in negative contrast due to large dark (nonfluorescent) lacunae, which probably reflect the presence of the hyphae of *P. viticola* in the host (Fig. 3C, arrow). This is also suggested by the sporangiophore (Fig. 3B, arrow) emerging from the stoma just above the dark structure (Fig. 3C, arrow). The limits of these lacunae display a brighter fluorescence and suggest that the development of *P. viticola* was inhibited. Aniline blue staining (Diez-Navajas *et al.*, 2007) of leaf sections confirmed the presence of mycelium in the mesophyll (not shown).

In vitro *spectrofluorimetry of stilbenes*

Three major physicochemical factors known to influence molecular fluorescence were tested: viscosity, polarity, and pH, at a controlled temperature of 20 °C.

Effect of viscosity: In viscous solution, the fluorescence yield of a fluorophore is increased due to the decrease of the rate of nonradiative dissipation (Valeur, 2001). As expected, increased viscosity induced an increase in fluorescence intensity in *trans*-resveratrol spectra accompanied by a hypochromic shift of the emission maximum from 400 nm in water to 386 nm in 100% glycerol (Fig. 4). This shift could be attributed to the lower polarity of this alcoholic solvent as compared to water. This result shows that viscosity has a critical influence on fluorescence yield, in this case a 137-fold increase, and has to be taken into account for interpretation of the variation of fluorescence intensity observed *in vivo*. Glycerol had a similar effect upon both *trans*-piceid and *trans*-pterostilbene (Supplementary Fig. S1).

Effect of solvent polarity and hydrogen bonding: Fluorophores are in general sensitive to solvent polarity, changing fluorescence quantum yield, and Stokes shift (Valeur, 2001). Six solvents of different polarities were chosen to dissolve *trans*-resveratrol (Fig. 5, Table 1). Generally, the higher the hydrogen bonding by a solvent, the higher the Stokes shift of fluorescence (Valeur, 2001). This is confirmed with the emission spectra of *trans*-resveratrol in water displaying a greater Stokes shift with maximum emission spectra at 400 nm in comparison to the other four protic solvents (also considering 100% glycerol) with a maximum around 380 nm (Figs. 4 and 5, Table 1). This bathochromic shift of stilbene fluorescence emission in water, also observed for *trans*-piceid and *trans*-pterostilbene (Supplementary Fig. S2), is explained by the strong hydrogen bonding of water and is a characteristic of an aqueous medium. In the six solvents analysed, a large variation of *trans*-resveratrol fluorescence intensity was observed, from 50 (water) to approximately 500 QSEU (propan-2-ol) (Fig. 5).

Effect of pH: Dissociation and proton transfer produce large effects on fluorescence. *Trans*-resveratrol exists in four

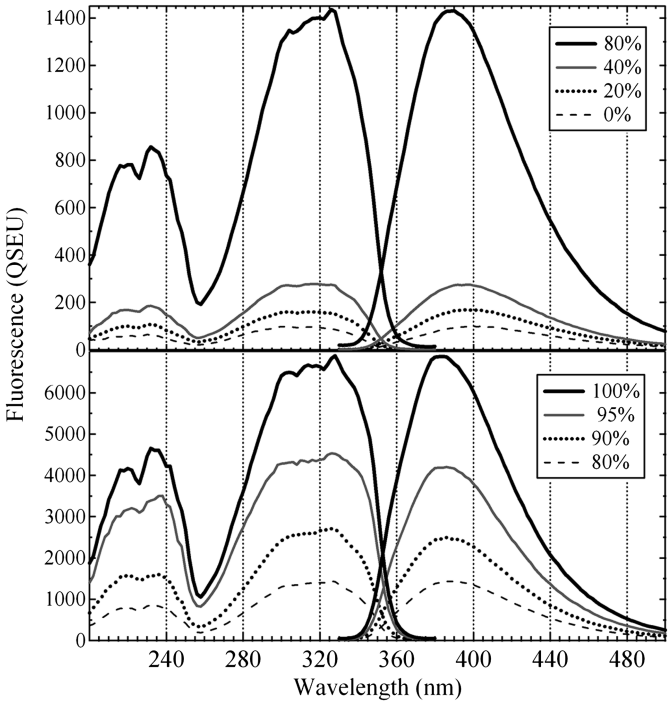

Fig. 4. Fluorescence spectra of *trans*-resveratrol (10 μM) in aqueous solutions at 20 °C with an increasing proportion of glycerol (v/v). The excitation spectra were acquired with an emission at 390 nm and the emission spectra were acquired with an excitation at 320 nm (maxima for *trans*-resveratrol in aqueous solutions). The full range of viscosity is presented in two graphs for better scaling. QSEU, quinine sulphate equivalent units (see Materials and methods). Correspondence of percentage glycerol and viscosity (cP): 0% = 1.002, 10% = 1.365, 20% = 1.986, 40% = 3.088; 80% = 84.34; 90% = 384.5; 95% = 780.5; 100% = 1490. See Supplementary Fig. S1 for analogous glycerol series in methanol, for *trans*-resveratrol, *trans*-piceid, and *trans*-pterostilbene.

tautomeric forms: the fully protonated form (neutral, noncharged), the mono-anionic form, the di-anionic form, and the tri-anionic form. *Trans*-resveratrol thus has three acidic-dissociation constants that determine the protonation state in solution at a given pH: pK_a1 = 8.01, pK_a2= 9.86, and pK_a3=10.5 (Lopez-Nicolas and Garcia-Carmona, 2008). Below pH 7, the noncharged form of *trans*-resveratrol is predominant and displays the characteristic emission spectrum with a band at 400 nm in water (Fig. 6). When pH becomes more basic, between pK_a1 and pK_a2, the noncharged and mono-anionic forms coexist. The fluorescence intensity gradually decreases displaying a peak at 400 nm and a shoulder at 460 nm corresponding to the contribution of the mono-anionic form (Fig. 6). When pH is at 9, the mono-anionic form is prevalent and its characteristic spectrum with a relative low fluorescence yield and a peak at 460 nm is observed (Fig. 6). At pH 10 (pK_a2), both mono-anionic and di-anionic forms coexist and a clear maximum intensity at 460 nm is observed (Fig. 6). At pH 11, the di-anionic and the tri-anionic forms coexist and the maximum emission band is still at 460 nm. At pH 12, the

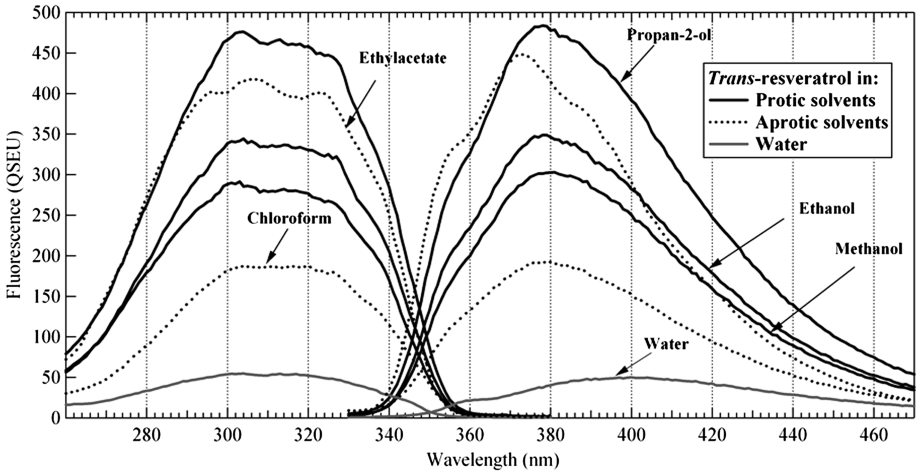

Fig. 5. Fluorescence spectra of *trans*-resveratrol (10 μM) in solvent of different polarity: water, methanol, ethanol, propan-2-ol, chloroform, and ethylacetate. Same experimental conditions as described in Fig. 4. See Supplementary Fig. S2 for analogous solvent series *with trans*-piceid and *trans*-pterostilbene.

Table 1. Characteristics of solvents used for fluorescence spectroscopy of *trans*-resveratrol
Emission maximum and peak intensity are extracted from Figs. 4 and 5.

Solvent	H-bonding	Dielectric constant	Viscosity at 20 °C (cP)[a]	Solvent cutoff (nm)	Emission maximum (nm)	Peak intensity (QSEU)
Chloroform	Aprotic	4.81[b]	0.58	245	379	193
Ethylacetate	Aprotic	6.02[a]	0.46	256	373	448
Propan-2-ol	Protic	20.0[a]	2.26	210	378	484
Ethanol	Protic	25.1[b]	1.20	210	378	349
Methanol	Protic	32.7[b]	0.59	205	381	303
Glycerol	Protic	42.5[a]	1490	207	386	6869
Water	Protic	80.1[a]	1.00	190	400	50

[a] Lide (2008)
[b] Valeur (2001).

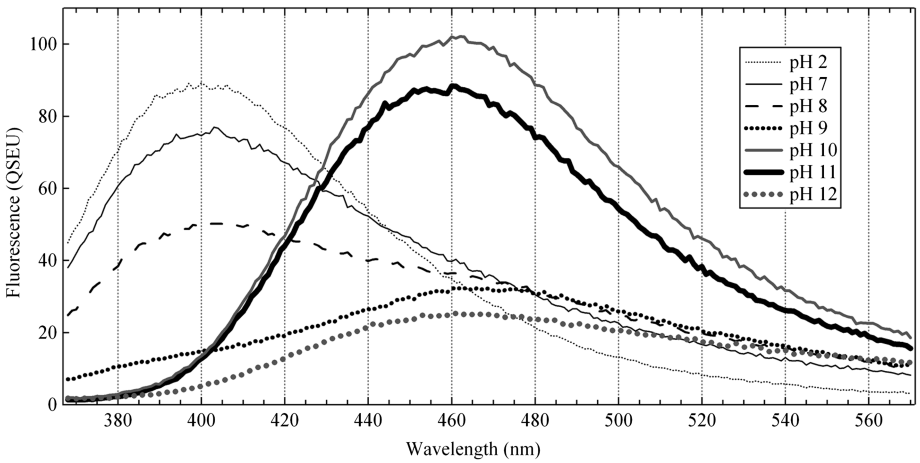

Fig. 6. Fluorescence emission spectra of aqueous solutions of trans-resveratrol (10 μM) with pH from 2 to 12. Same experimental conditions as described in Fig. 4. See Supplementary Fig. S3 for analogous pH series with *trans*-piceid and *trans*-pterostilbenes.

tri-anionic form is predominant: this has the lowest fluorescence yield and displays a maximum at 460 nm. The same experiment was done with *trans*-pterostilbene and *trans*-piceid. Although piceid has only two pK_a and pterostilbene only one, the results were the same except that the position of the second peak was shifted to 455 nm for piceid and to 470 nm for pterostilbene (Supplementary Fig. S3). In all cases, the first peak of the noncharged form was located at 400 nm. The pH of the various solvents used in the preceding section (Figs. 4 and 5) were below 8, so below pK_a1.

Discussion

Localization of stilbene autofluorescence on infected leaves

Prior to this study, few reports on the *in vivo* localization of stilbenes were available despite the interest drawn by this class of stress metabolites. Dai *et al.* (1995a, b) reported in several histochemical studies the presence of autofluorescence of stilbenes in diffuse necrotic areas immediately around the infected guard cells. The elicitor-induced formation of cell-wall-bound stilbenes has been described in cell-suspension cultures of Scots pine (Lange *et al.*, 1994) and experiments on *V. vinifera* cell-suspension suggested that stilbenes could, by binding to cell walls, contribute to their chemical reinforcement in response to stresses (Lesniewska *et al.*, 2004; Adrian *et al.*, 2006). Poutaraud *et al.* (2007) observed the increase of blue fluorescence in abaxial and adaxial cell walls and veins. The present observation of the autofluorescence of stilbenes in cutinized cell walls (outer periclinal cell walls of epidermal cells, especially outer periclinal and anticlinal junctions, and entire cell walls of guard cells) confirms these results. Poutaraud *et al.* (2010) pointed out that stilbenes produced in inner leaf tissues are unlikely to be detectable by standard fluorimetry, hence explaining the small differences observed between susceptible, partially resistant, and totally resistant genotypes in the correlation between fluorescence and HPLC measurements of stilbenes. The *in situ* visualization of stilbene autofluorescence in vacuoles of epidermal cells and in the spongy mesophyll of grapevine leaves, achieved in the present report, has no precedent and confirms the presence of stilbenes in the inner leaf tissues. It is in good agreement with the *ex situ* observations realized so far, notably: protoplasts of grapevine leaves were shown to exhibit a bright blue fluorescence under UV-excitation due to stilbenes (Commun *et al.*, 2003) and an accumulation of piceids within cells (probably in vacuoles) was observed *in vitro* on cell-suspensions submitted to elicitation (Donnez *et al.*, 2011) while *trans*-resveratrol is mainly released in the culture medium (Donnez *et al.*, 2009). *Trans*-resveratrol release has also been described in *Vitis* leaves (Blaich and Bachmann, 1980) under stress conditions. The spectral comparison between inoculated and control samples, in addition to previous macroscopic scale experiments (Poutaraud *et al.*, 2007, 2010), allowed the present study to ascertain, at a microscopic scale, the contribution of stilbene fluorescence wherever new BGF was observed.

Emission spectra of grapevine leaves were acquired with the shorter UV laser band available on the microscope, 351 nm. Unfortunately, this was far from the maximum excitation wavelength for stilbenes, between 300 and 330 nm. Moreover, 351-nm light excited well the fluorescence of constitutive hydroxycinnamic acids already present in noninoculated leaves. This compromise on specificity of excitation and the very high spatial resolution ($0.15 \times 0.15 \times 0.38$ μm for x, y, and z directions respectively) may explain differences observed in emission spectra of leaves between this microspectrofluorimetric study and previous investigations at a macroscopic scale that offered total choice of excitation and emission bands (Poutaraud *et al.*, 2007). Furthermore, it is worth noting that it is not possible to discriminate among the different type of stilbenes involved. Indeed, natural stilbenes induced in grapevine leaves share very close fluorescence emission spectra (Poutaraud *et al.*, 2007) and yields (Supplementary Figs. S1–3). Imaging by mass spectrometry would provide the information on the nature and the localization of stilbenes simultaneously, but not *in vivo* and with a low resolution where leaf structures are not resolved, nor is depth achieved (Hamm *et al.*, 2010).

These *in vitro* spectrofluorimetric results show that the rigidity of the compartment is the most critical physicochemical factor in addition to concentration, influencing the fluorescence yield of stilbenes *in vivo*, while the hydrogen bonding and the polarity generated by the medium have a much lower influence on the fluorescence yield but can modify the Stokes shift. Thus, the fact that the fluorescence intensity of stilbenes was higher in GC cell walls than in mesophyll, for example, does not necessarily mean a higher concentration of fluorophores, but may just be due to the higher rigidity of the highly cutinized environment of GC. Plant tissues are formed of cells containing compartments (and microenvironments) with extreme variations of rigidity and fluidity. Natural fluorophores like stilbenes will actually be probes of local viscosity, which influence their fluorescence intensity as much as their concentration does. Viscosity in the vacuole must be close to that of a 5% solution of small molecules and electrolytes, say 1.12 cP (equivalent to 5% glycerol). Suhling *et al.* (2004) measured an average cytoplasmic viscosity of 2–6 cP (equivalent to 24–52% glycerol), reporting point measures from 1.2 to 10 cP (citations therein). The cuticular waxes and cutinized cell walls must offer viscosities far above that of pure glycerol. So plant tissue compartments constitute environments where fluorescence yield of stilbenes must vary at least 140-fold (much like in Fig. 4) between the vacuole or the cytoplasm and the cell walls or waxes. The pH would never exceed 7.5 in cytosol (Bligny *et al.*, 1997). The minimal pH is usually found in the vacuole with 5.5 (Bligny *et al.*, 1997) and the pH of apoplasm is around 6.5 within the substomatal cavity (Felle and Hanstein, 2002). In other words, under normal physiological conditions only the fully protonated form of stilbene is present and its fluorescence would not be modulated by any pH shifts comparable to the *in vitro* study. The shift of the emission peak from 400 to 430 nm seen in vacuoles (Fig. 2C) can be the consequence of the bathochromic shift of the fluorescence emission maximum of stilbenes in an aqueous environment compared to a nonaqueous one (Fig. 5). Alternatively, an increase of the pH due to the presence of the pathogen in these structures would lead to a similar bathochromic shift of the fluorescence emission spectrum (see pH 9 in Fig. 6), which would apply also to infected EC cell walls. This question needs further investigations, namely the measurement of the local pH *in vivo*.

Localization of stilbene phytoalexins and host interaction

A recent ultrastructural study recalled that *P. viticola* infections on resistant genotypes are restricted to the upper part of the loose spongy mesophyll and are associated with rapid both mycelium and mesophyll cell-wall disruption (Alonso-Villaverde *et al.*, 2011). Kortekamp *et al.* (1998), in a similar investigation of the interaction of *P. viticola* with the host, had observed that the morphologic degeneration of the mycelium in resistant tissues started as early as 3 dpi. A histochemical study of the host and nonhost resistance to downy mildew underlined the central role of haustoria in the establishment of biotrophic parasitism and in the induction of a hypersensitive response (Diez-Navajas *et al.*, 2008). During the haustorium formation, fungal hyphae and plant cells come in close contact (Kortekamp *et al.*, 1998). Mature haustoria were never observed in nonhost species. On the other hand, in both resistant and susceptible grapevine tissues, fully developed haustoria were visible, which indicate that activation of effective defence responses depends on the haustoria–mesophyll cells' interaction (Diez-Navajas *et al.*, 2008). Langcake and Lovell (1980), in their ultrastructural study, reported two types of response at the later stages of infection suggesting also a triggering of active defences in the mesophyll by haustoria. In susceptible genotypes, they observed the degeneration of the cytoplasm of host cells while the haustorium retained its normal appearance. In resistant genotypes, they reported incomplete cytoplasm degeneration and collapse of haustoria with adjacent intercellular hyphae remaining apparently healthy. The present observations on the localization of stilbene fluorescence confirm their induction in epidermal and guard-cell walls of all genotypes, susceptible and partially resistant. Stilbenes released and located in cutinized layers of the apoplast have probably a low or no efficiency in terms of toxicity against *P. viticola*, which is located in the mesophyll. Interestingly, this study observed a correlation between higher resistance levels and stilbene localization. While stilbene fluorescence was seen only in epidermal and guard-cell cutinized walls for the very susceptible genotype Muscat Ottonel, Cabernet Sauvignon (susceptible genotype) displayed the presence of induced stilbenes in epidermal cell vacuoles and, above all, RV1 (partially resistant genotype) displayed their presence pretty much everywhere in the spongy parenchyma (intercellular space and/or vacuoles of the mesophyll). Even if these results by themselves do not address the role of stilbenes in the growth inhibition of *P. viticola* in the spongy mesophyll, the fact that ultrastructural studies reported mycelial cell destruction concomitant to expulsion of mycelial cell content around haustoria in the case of resistant genotypes (Alonso-Villaverde *et al.*, 2011) strongly suggest that stilbenes are involved in the process.

Conclusion

Imaging and comparative spectral analysis of stilbene fluorescence *in vivo* revealed the presence of these phytoalexins in the mesophyll of a partially resistant grapevine genotype, a presence probably underestimated because of the microenvironement dependency of fluorescent yield. It is in this very tissue that the inhibition of *P. viticola* mycelium apparently occurs, but a causal relationship with phytoalexins has yet to be shown *in vivo*. Nevertheless, confocal microscopy coupled to microspectrofluorimetry offers enough resolution to localize and characterize intrinsic fluorophores in leaf tissues. Fluorescence imaging appears more than ever the noninvasive method of choice to evaluate the local presence of different compounds. *In vivo* 3D confocal imaging of autofluorescence of stilbenes in epidermal and mesophyll cells could be of interest in screening for disease resistance of grapevine in breeding programmes. Such an analytical tool is also an essential prerequisite for the development of fluorescence sensors for detection of diseases straight in the field.

Supplementary material

Supplementary data are available at *JXB* online.

Supplementary Video S1. Animated version of Fig. 1A, B.

Supplementary Video S2. Animated version of Fig. 1E, F.

Supplementary Video S3. Animated version of Fig. 1I, J.

Supplementary Video S4. Animated version of Fig. 3C.

Supplementary Fig. S1. Fluorescence spectra of *trans*-resveratrol, *trans*-piceid, and *trans*-pterostilbene in methanolic solutions (10 μM) with an increasing proportion of glycerol.

Supplementary Fig. S2. Fluorescence emission spectra of aqueous solution of *trans*-resveratrol (from Fig. 6), *trans*-piceid, and *trans*-pterostilbene (10 μM) with pH 7–12.

Supplementary Fig. S3. Fluorescence spectra of *trans*-resveratrol (from Fig. 5), *trans*-piceid, and *trans*-pterostilbene (10 μM) in solvents of different polarity.

Acknowledgements

This work was supported by Force-A (Orsay) in a joint project with Centre National de la Recherche Scientifique (CNRS), Institut National de la Recherche Agronomique (INRA), and Université Paris-Sud 11 (UPS) (grant numbers CNRS 065103, INRA 28000039, and UPS N73800) and by Institut Fédératif de Recherche 87 *La plante et son environnement* (grant number IFR87).

The Zeiss confocal microscope belongs to Institut de Neurobiologie Alfred Fessard (Gif-sur-Yvette, France) and we thank immensely José Cancela and Sandrine Guyon (NBCM) for access to this equipment. The Imagif Platform served for support observations, and we thank Marie-Noëlle Soler (IFR87). We are grateful to Marie Annick Dorne and Pascale Coste (INRA, Colmar) for growing the grapevine plants and their inoculation and to Sabine Merdinoglu and Didier Merdinoglu (INRA, Colmar) for their support.

References

Adrian M, Lesniewska E, Allègre M, Pugin A. 2006. Physical and chemical aspects of grapevine cell wall strengthening following activation of defense reactions. In: Jeandet P, Clément C, Conreux A, eds, *Macrowine 2006. Macromolecules and Secondary metabolites of Grapevine and Wines*. Reims: University of Reims, 75–82.

Alonso-Villaverde V, Voinesco F, Viret O, Spring JL, Gindro K. 2011. The effectiveness of stilbenes in resistant *Vitaceae*: ultrastructural and biochemical events during *Plasmopara viticola* infection process. *Plant Physiology and Biochemistry* **49,** 265–274.

Blaich R, Bachmann O. 1980. The resveratrol synthesis in Vitaceae induction and cytological observations. *Vitis* **19,** 230–240.

Bligny R, Gout E, Kaiser W, Heber U, Walker D, Douce R. 1997. pH regulation in acid-stressed leaves of pea plants grown in the presence of nitrate or ammonium salts: studies involving P-31-NMR spectroscopy and chlorophyll fluorescence. *Biochimica Et Biophysica Acta* **1320,** 142–152.

Cerovic ZG, Samson G, Morales F, Tremblay N, Moya I. 1999. Ultraviolet-induced fluorescence for plant monitoring: present state and prospects. Agronomie: *Agriculture and Environment* **19,** 543–578.

Chong J, Poutaraud A, Hugueney P. 2009. Metabolism and roles of stilbenes in plants. *Plant Science* **177,** 143–155.

Commun K, Mauro MC, Chupeau Y, Boulay M, Burrus M, Jeandet P. 2003. Phytoalexin production in grapevine protoplasts during isolation and culture. *Plant Physiology and Biochemistry* **41,** 317–323.

Dai GH, Andary C, Mondolot-Cosson L, Boubals D. 1995*a*. Histochemical studies on the interaction between three species of grapevine, *Vitis vinifera, V. rupestris, V. rotundifolia* and the downy mildew fungus. *Physiological and Molecular Plant Pathology* **46,** 177–188.

Dai GH, Andary C, Mondolot-Cosson L, Boubals D. 1995*b*. Histochemical responses of leaves of *in-vitro* plantlets of *Vitis* spp to infection with *Plasmopara viticola*. *Phytopathology* **85,** 149–154.

Dercks W, Creasy LL. 1989. The significance of stilbene phytoalexins in the *Plasmopara viticola* grapevine interaction. *Physiological and Molecular Plant Pathology* **34,** 189–202.

Diez-Navajas AM, Greif C, Poutaraud A, Merdinoglu D. 2007. Two simplified fluorescent staining techniques to observe infection structures of the oomycete *Plasmopara viticola* in grapevine leaf tissues. *Micron* **38,** 680–683.

Diez-Navajas AM, Wiedemann-Merdinoglu S, Greif C, Merdinoglu D. 2008. Nonhost versus host resistance to the grapevine downy mildew, *Plasmopara viticola*, studied at the tissue level. *Phytopathology* **98,** 776–780.

Donnez D, Jeandet P, Clement C, Courot E. 2009. Bioproduction of resveratrol and stilbene derivatives by plant cells and microorganisms. *Trends in Biotechnology* **27,** 706–713.

Donnez D, Kim KH, Antoine S, Conreux A, De Luca V, Jeandet P, Clement C, Courot E. 2011. Bioproduction of resveratrol and viniferins by an elicited grapevine cell culture in a 2 L stirred bioreactor. *Process Biochemistry* **46,** 1056–1062.

Felle HH, Hanstein S. 2002. The apoplastic pH of the substomatal cavity of *Vicia faba* leaves and its regulation responding to different stress factors. *Journal of Experimental Botany* **53,** 73–82.

Fornara V, Onelli E, Sparvoli F, Rossoni M, Aina R, Marino G, Citterio S. 2008. Localization of stilbene synthase in *Vitis vinifera* L. during berry development. *Protoplasma* **233,** 83–93.

Gindro K, Spring JL, Pezet R, Richter H, Viret O. 2006. Histological and biochemical criteria for objective and early selection of grapevine cultivars resistant to *Plasmopara viticola*. *Vitis* **45,** 191–196.

Hamm G, Carre V, Poutaraud A, Maunit B, Frache G, Merdinoglu D, Muller JF. 2010. Determination and imaging of metabolites from *Vitis vinifera* leaves by laser desorption/ionisation time-of-flight mass spectrometry. *Rapid Communications in Mass Spectrometry* **24,** 335–342.

Hammerschmidt R. 1999. Phytoalexins: what have we learned after 60 years? *Annual Review of Phytopathology* **37,** 285–306.

Harborne JB. 1999. *The Comparative Biochemistry of Phytoalexin Induction in Plants*. Kidlington, UK: Elsevier.

Hillis WE, Ishikura N. 1968. Chromatographic and spectral properties of stilbene derivatives. *Journal of Chromatography* **32,** 323–336.

Hoos G, Blaich R. 1990. Influence of resveratrol on germination of conidia and mycelial growth of *Botrytis cinerea* and *Phomopsis viticola*. *Journal of Phytopathology* **129,** 102–110.

Hutzler P, Fischbach R, Heller W, Jungblut TP, Reuber S, Schmitz R, Veit M, Weissenbock G, Schnitzler JP. 1998. Tissue localization of phenolic compounds in plants by confocal laser scanning microscopy. *Journal of Experimental Botany* **49,** 953–965.

Jaillon O, Aury JM, Noel B, *et al*. 2007. The grapevine genome sequence suggests ancestral hexaploidization in major angiosperm phyla. *Nature* **449,** 463–U465.

Jeandet P, Bessis R, Sbaghi M, Meunier P. 1995. Production of the phytoalexin resveratrol by grapes as a response to *Botrytis* attack under natural conditions. *Journal of Phytopathology* **143,** 135–139.

Kortekamp A, Wind R, Zyprian E. 1998. Investigation of the interaction of *Plasmopara viticola* with susceptible and resistant grapevine cultivars. *Journal of Plant Diseases and Protection* **105,** 475–488.

Kuc J. 1995. Phytoalexins, stress metabolism, and disease resistance in plants. *Annual Review of Phytopathology* **33,** 275–297.

Langcake P. 1981. Disease resistance of *Vitis* spp. and the production of the stress metabolites resveratrol, ϵ-viniferin, α-viniferin, and pterostilbene. *Physiological Plant Pathology* **18,** 213–226.

Langcake P, Cornford CA, Pryce RJ. 1979. Identification of pterostilbene as a phytoalexin from *Vitis vinifera* leaves. *Phytochemistry* **18,** 1025–1027.

Langcake P, Lovell PA. 1980. Light and electron microscopical studies of the infection of *Vitis* spp. by *Plasmopara viticola*, the downy mildew pathogen. *Vitis* **19,** 321–337.

Langcake P, Pryce RJ. 1976. Production of resveratrol by *Vitis vinifera* and other members of *Vitaceae* as a response to infection or injury. *Physiological Plant Pathology* **9,** 77–86.

Langcake P, Pryce RJ. 1977. New class of phytoalexins from grapevines. *Experientia* **33,** 151–152.

Lange BM, Trost M, Heller W, Langebartels C, Sandermann H. 1994. Elicitor induced formation of free and cell-wall bound stilbenes in

cell-suspension cultures of Scots Pine (*Pinus Sylvestris*). *Planta* **194,** 143–148.

Lesniewska E, Adrian M, Klinguer A, Pugin A. 2004. Cell wall modification in grapevine cells in response to UV stress investigated by atomic force microscopy. *Ultramicroscopy* **100,** 171–178.

Lide DR. 2008. *CRC Handbook of Chemistry and Physics: a ready-reference book of chemical and physical data*. Boca Raton: CRC Press.

Lopez-Nicolas JM, Garcia-Carmona F. 2008. Aggregation state and pK(a) values of (E)-resveratrol as determined by fluorescence spectroscopy and UV-visible absorption. *Journal of Agricultural and Food Chemistry* **56,** 7600–7605.

Louis J, Cerovic ZG, Moya I. 2006. Quantitative study of fluorescence excitation and emission spectra of bean leaves. *Journal of Photochemistry and Photobiology B, Biology* **85,** 65–71.

Merdinoglu D, Wiedemann-Merdinoglu S, Coste P, Dumas V, Haetty S, Butterlin G, Greif C. 2003. Genetic analysis of downy mildew resistance derived from *Muscadinia rotundifolia*. In: Hajdu E, Borbas E, eds, *Proceedings of the 8th International Conference on Grape Genetics and Breeding*, vols. 1 and 2. Leuven 1: International Society Horticultural Science, 451–456.

Meyer S, Cartelat A, Moya I, Cerovic ZG. 2003. UV-induced blue-green and far-red fluorescence along wheat leaves: a potential signature of leaf ageing. *Journal of Experimental Botany* **54,** 757–769.

Pezet R, Gindro K, Viret O, Richter H. 2004*a*. Effects of resveratrol, viniferins and pterostilbene on *Plasmopara viticola* zoospore mobility and disease development. *Vitis* **43,** 145–148.

Pezet R, Gindro K, Viret O, Spring JL. 2004*b*. Glycosylation and oxidative dimerization of resveratrol are respectively associated to sensitivity and resistance of grapevine cultivars to downy mildew. *Physiological and Molecular Plant Pathology* **65,** 297–303.

Pezet R, Perret C, Jean-Denis JB, Tabacchi R, Gindro K, Viret O. 2003. Delta-viniferin, a resveratrol dehydrodimer: one of the major stilbenes synthesized by stressed grapevine leaves. *Journal of Agricultural and Food Chemistry* **51,** 5488–5492.

Pezet R, Pont V, Cuenat P. 1994. Method to determine resveratrol and pterostilbene in grape berries and wines using high-performance liquid chromatography and highly sensitive fluorimetric detection. *Journal of Chromatography A* **673,** 191–197.

Pfündel EE, Agati G, Cerovic ZG. 2006. Optical properties of plant surfaces. In: Reiderer M, üller CM, eds, *Biology of the Plant Cuticle*, vol. 23. Oxford: Blackwell Publishing, 216–249.

Pool RM, Creasy LL, Frackelton AS. 1981. Resveratrol and the viniferins, their application to screening for disease resistance in grape breeding programs. *Vitis* **20,** 136–145.

Poutaraud A, Latouche G, Cerovic ZG, Merdinoglu D. 2010. Quantification of stilbene in grapevine leaves by direct fluorometry and high performance liquid chromatography: spatial localisation and time course of synthesis. *Journal International des Sciences de la Vigne et du Vin, Special Issue Macrowine* **44,** 27–32.

Poutaraud A, Latouche G, Martins S, Meyer S, Merdinoglu D, Cerovic ZG. 2007. Fast and local assessment of stilbene content in grapevine leaf by *in vivo* fluorometry. *Journal of Agricultural and Food Chemistry* **55,** 4913–4920.

Schnee S, Viret O, Gindro K. 2008. Role of stilbenes in the resistance of grapevine to powdery mildew. *Physiological and Molecular Plant Pathology* **72,** 128–133.

Shiraishi M, Chijiwa H, Fujishima H, Muramoto K. 2010. Resveratrol production potential of grape flowers and green berries to screen genotypes for gray mold and powdery mildew resistance. *Euphytica* **176,** 371–381.

Suhling K, Siegel J, Lanigan PMP, Leveque-Fort S, Webb SED, Phillips D, Davis DM, French PMW. 2004. Time-resolved fluorescence anisotropy imaging applied to live cells. *Optics Letters* **29,** 584–586.

Valeur B. 2001. *Molecular Fluorescence*. Weinheim: Wiley.

Vance CP, Kirk TK, Sherwood RT. 1980. Lignification as a mechanism of disease resistance. *Annual Review of Phytopathology* **18,** 259–288.

Wang W, Tang K, Yang HR, Wen PF, Zhang P, Wang HL, Huang WD. 2010. Distribution of resveratrol and stilbene synthase in young grape plants (*Vitis vinifera* L. cv. Cabernet Sauvignon) and the effect of UV-C on its accumulation. *Plant Physiology and Biochemistry* **48,** 142–152.